Bioorganic Chemistry xxx (xxxx) xxxx

Contents lists available at ScienceDirect

Bioorganic Chemistry

journal homepage: www.elsevier.com/locate/bioorg

Synthesis and discovery of pyrazolo-pyridine analogs as inflammation medications through pro- and anti-inflammatory cytokine and COX-2 inhibition assessments

J. Dennis Bilavendran[a], A. Manikandan[b,*], P. Thangarasu[a], K. Sivakumar[a,c,*]

[a] Research and Development Centre, Bharathiar University, Coimbatore 641046, India
[b] Department of Biotechnology, School of Bio-Sciences and Technology, VIT University, Vellore 632014, India
[c] Department of Chemistry, Adhiyamaan College of Engineering, Hosur 635109, India

ARTICLE INFO

Keywords:
Anti-inflammation
COX-2
IL-1 β
IL-10
Inflammatory cytokines
Molecular docking
Pyrazolopyridines

ABSTRACT

This article briefs about the efforts taken to synthesis, characterize and develop (E)-5-methyl-2-phenyl-3-(thiophen-2-yl)-7-(thiophen-2-ylmethylene)-3,3a,4,5,6,7-hexahydro-2H-pyrazolo[4,3-*c*]pyridine and their analogs. In the two-step reaction, the first step is the synthesis of (3Z,5E)-1-methyl-3,5-bis(thiophen-2-ylmethylene) piperidin-4-one derivatives (**3a-l**) by stirring the mixture of 1-methylpiperidin-4-one and substituted thiophene-carbaldehydes in presence of methanol. In the second and final step, compounds **3a-l** were refluxed with phenyl-hydrazine to achieve the target compounds (E)-5-methyl-2-phenyl-3-(thiophen-2-yl)-7-(thiophen-2-ylmethylene)-3,3a,4,5,6,7-hexahydro-2H-pyrazolo[4,3-*c*]pyridine and their analogs (**5a-l**) in good yield. These compounds were used to assess their inflammation regulation properties in macrophages by executing quantitative pro-inflammatory and anti-inflammatory proteins such as TNF-α, IL-1β, IL6, and IL-10 respectively. *In silico* and *in vitro* COX-2 inhibition studies helped to understand the molecular interaction or plausible mechanism during the inflammation regulation that showed by the compounds. In the results, among the 12-member family of pyrazolo-pyridines (**5a-l**), **5a**, **5b**, **5g,** and **5j** were showed excellent *in silico* binding affinity (1–10 nM), least binding energy (−12.45 to −14.27 kcal/mol) and *in vitro* COX-2 inhibition (relative percentage activity maximum 96.42%). Thus, these compounds perhaps to be future anti-inflammatory drugs.

1. Introduction

The present research deals about the design synthesis and finding the pyrazolo-pyridine based analogs as inflammation medications through the analysis and assessment of pro- and anti-inflammatory cytokine expressed in macrophages and COX-2 enzyme inhibition assessments. Among a range of druggable pyridine based small molecule entities, pyrazolopyridines take an important place as they have been widely assessed as antimicrobial [1], anti-cancer [2–4], etc. Pyrazolopyridines are used to treat anxiolytics which act as positive allosteric modulators of the $GABA_A$ receptor [5]. Fig. 1 representing a few existing pyrazolopyridines based drug adjuvants and the comparison with the present study compound **5g**. The designed and synthesized pyrazolopyridines (**5a-l**) were assessed for the anti-inflammatory activity potential as predicted from online bioactivity prediction tools such as molinspiration (molinspiration.com/) and PASSonline (www.pharmaexpert.ru/passonline/).

Inflammation is an immune response of the body. In fact, inflammation itself a disease also being the gateway for many diseases [6]. Acute inflammation becomes chronic when inflammation prolongs [7]. Thus the so-called “false alarms” linking chronic inflammation and most of the autoimmune disorders [8]. Chronic inflammation can ultimately cause numerous diseases and disorders, including some cancers and rheumatoid arthritis [9]. Non-steroidal anti-inflammatory drugs (NSAIDs) are prescribed to alleviate the pain instigated from inflammation. NSAIDs either prevents or reduces pain and naproxen, ibuprofen, and aspirin are the examples [10,11]. They counteract the isoforms of cyclooxygenase (COX 1 & COX 2) enzyme that mainly involved in the development of inflammation [10–12]. In cells, COX 1 & COX 2 enzymes are mainly involved in the synthesis of key biological inflammation mediators, namely prostaglandins (PGs) [12,13]. PGs are highly involved in inflammation, and thromboxanes that are crucial in blood clotting [13].

Inflammation mostly characterized by a back-and-forth interaction

* Corresponding authors at: Research and Development Centre, Bharathiar University, Coimbatore 641046, India (K. Sivakumar).
E-mail addresses: mailtomicromani@gmail.com (A. Manikandan), siva1782@gmail.com (K. Sivakumar).

https://doi.org/10.1016/j.bioorg.2019.103484
Received 6 August 2019; Received in revised form 8 September 2019; Accepted 26 November 2019

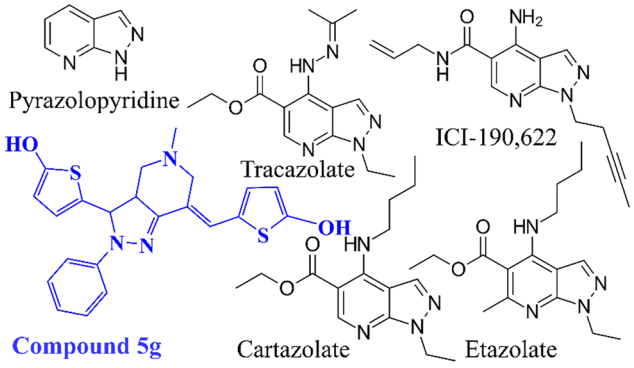

Fig. 1. Comparison of present study compound **5g** with Pyrazolopyridine based drug moieties.

between pro-inflammatory and anti-inflammatory cytokines. Interleukin-1 (IL-1), Interleukin-1β (IL-1β), Tumor Necrosis Factor-alpha (TNF-α), gamma-interferon (IFN-gamma), IL-6, IL-12, IL-18, granulocyte-macrophage colony-stimulating factor (G-MCSF) and are well categorized as pro-inflammatory cytokines whereas IFN-alpha, IL4, IL-10, IL-13, and transforming growth factor-beta (TGF-β) are renowned as anti-inflammatory cytokines [14–16]. In this study, Pyrazolopyridine based 12 derivatives (**5a-l**) were used as the anti-inflammatory candidate drugs and the pro-inflammatory IL-1β, IL-6, TNF-α, and anti-inflammatory IL-10 molecules were assessed before and after the treatment of these compounds in macrophages.

In another *in vitro* anti-inflammation assessment, (Human Red-blood Cells) HRBC based membrane stabilization study for pyrazolopyridines (**5a-l**) was accomplished. HRBC is alike lysosomal membrane and supposed to inhibit the inflammation development by controlling the release of corresponding lysosomal enzymes. Various range of substances that are discharged by a lysosomal enzyme in the progression of inflammation-causing multiple disorders. This extracellular activity is known as acute or chronic inflammation [17–19]. Apart from this major investigation, we have also assessed the molecular interaction of pyrazolopyridines (**5a-l**) through molecular docking and *in vitro* COX-2 inhibition.

2. Materials and methods

Chemistry: All organic chemicals and reagents procured from Sigma-Aldrich, Spectrochem, and Avra. Solvents and reagents were used as received by not doing further purification. For thin-layer chromatography (TLC) analysis, Merck pre-coated silica plates (Silica gel 60 F254) were used and spots visualized under UV light. Redisep silica gel columns used for flash chromatography and mobile phase solvents as indicated in procedures. ^{1}H NMR and ^{13}C NMR recorded in Bruker-400 MHz instrument. LC-MS recorded on Agilent instruments.

2.1. Synthesis of (3Z,5E)-1-methyl-3,5-bis(thiophen-2-ylmethylene) piperidin-4-one derivatives (3a-l)

A mixture of 0.01 mol 1-methylpiperidin-4-one (**1**) and 0.02 mol substituted thiophene-carbaldehydes (**2**) in 15 ml of methanol was stirred at room temperature for 15 min. With this, 5 mol% NaOH was added dropwise. The progression and completion of reaction was monitered by TLC. After the reaction completed, the obtained solid obtained was filtered and washed with water. The crude product obtained was recrystallized using EtOH and THF in 1:1 ratio. The obtained product (**3**) was used as starting material for the synthesis of target compounds **5a-l**.

2.1.1. Characterization of (3Z,5E)-1-methyl-3,5-bis(thiophen-2-ylmethylene) piperidin-4-one derivatives (3a-l)

(3Z,5E)-1-methyl-3,5-bis(thiophen-2-ylmethylene)piperidin-4-one (3a): Yellow powder; Melting point: 99–101 °C: IR (KBr): 3012, 2345, 1712, 1518, 1345, 1202, 752, 640 cm^{-1}: ^{1}H NMR (400 MHz, $CDCl_3$) δ ppm: 8.10 (d, J = 8.0 Hz, 2H), 7.81 (d, J = 4.0 Hz, 2H), 7.58 (s, 1H), 7.40–7.38 (d, J = 3.6 Hz, 2H), 7.12 (s, 1H), 3.81 (d, J = 4.0 Hz, 4H), 2.27 (s, 3H); ^{13}C NMR (100 MHz, $CDCl_3$) δ ppm: 184.1, 146.8, 141.9, 140.8, 137.8, 137.1, 137.0, 130.6, 130.5, 129.2, 129.1, 128.3, 128.0, 64.1, 56.8, 42.9; HRMS for $C_{16}H_{15}NOS_2$ Calculated [M$^+$] m/z 301.4220, Found 301.4224.

(3Z,5E)-1-methyl-3,5-bis(thiophen-3-ylmethylene)piperidin-4-one(3b): Brown solid; Melting point: 102–104 °C: IR (KBr): 3008, 2368, 1724, 1567, 1327, 1234, 780, 664 cm^{-1}: ^{1}H NMR (400 MHz, $CDCl_3$) δ ppm: 7.83 (d, J = 4.0 Hz, 4H), 7.62 (s, 1H), 7.28–7.22 (m, 2H), 7.12 (s, 1H), 3.37 (d, J = 4.0 Hz, 4H), 2.28 (s, 3H); ^{13}C NMR (100 MHz, $CDCl_3$) δ ppm: 184.8, 146.7, 141.8, 140.1, 137.2, 137.0, 136.9, 130.2, 130.4, 129.1, 129.0, 128.8, 128.7, 64.3, 56.1, 43.1; HRMS for $C_{16}H_{15}NOS_2$ Calculated [M$^+$] m/z 301.4220, Found 301.4220.

(3Z,5E)-3,5-bis((5-bromothiophen-2-yl)methylene)-1-methylpiperidin-4-one (3c): Yellow solid; Melting point: 128–130 °C: IR (KBr): 3122, 2364, 1820, 1712, 1532, 1318, 1234, 780, 664 cm^{-1}: ^{1}H NMR (400 MHz, $CDCl_3$) δ ppm: 7.62–7.58 (m, 3H), 7.27 (d, J = 8.0 Hz, 2H), 7.13 (s, 1H), 3.41 (d, J = 4.0 Hz, 4H), 2.29 (s, 3H); ^{13}C NMR (100 MHz, $CDCl_3$) δ ppm: 186.2, 146.2, 142.0, 141.0, 138.1, 136.9, 137.0, 131.0, 130.9, 129.8, 129.7, 128.1, 128.0, 110.0, 64.5, 56.4, 42.2; HRMS for $C_{16}H_{13}Br_2NOS_2$ Calculated [M$^+$] m/z 459.2140, Found 459.2144.

(3Z,5E)-3,5-bis((5-chlorothiophen-2-yl)methylene)-1-methylpiperidin-4-one (3d): Deep yellow powder; Melting point: 108–110 °C: IR (KBr): 2998, 2389, 1814, 1748, 1547, 1345, 1202, 758, 642 cm^{-1}: ^{1}H NMR (400 MHz, $CDCl_3$) δ ppm: 7.86 (d, J = 8.0 Hz, 3H), 7.9 (d, J = 8.0 Hz, 3H), 3.37 (d, J = 4.0 Hz, 4H), 2.28 (s, 3H); ^{13}C NMR (100 MHz, $CDCl_3$) δ ppm: 183.2, 144.6, 139.4, 138.8, 136.1, 135.9, 135.0, 131.2, 130.0, 129.8, 129.0, 128.5, 128.4, 64.2, 56.1, 42.4; HRMS for $C_{16}H_{13}Cl_2NOS_2$ Calculated [M$^+$] m/z 370.3060, Found 370.3066.

(3Z,5E)-3,5-bis((5-fluorothiophen-2-yl)methylene)-1-methylpiperidin-4-one (3e): Deep yellow solid; Melting point: 102–104 °C: IR (KBr): 3018, 2349, 1728, 1527, 1356, 1257, 784, 667 cm^{-1}: ^{1}H NMR (400 MHz, $CDCl_3$) δ ppm: 7.60 (s, 1H), 7.52–7.48 (m, 2H), 7.13 (s, 1H), 6.71 (t, J = 8.0 Hz, 2H), 3.37 (d, J = 8.0 Hz, 4H), 2.28 (s, 3H); ^{13}C NMR (100 MHz, $CDCl_3$) δ ppm: 184.1, 146.8, 141.9, 140.8, 137.8, 137.1, 137.0, 130.6, 130.5, 129.2, 129.1, 128.3, 128.0, 64.1, 56.8, 42.9; HRMS for $C_{16}H_{13}F_2NOS_2$ Calculated [M$^+$] m/z 337.4028, Found 337.4031.

(3Z,5E)-1-methyl-3,5-bis((5-methylthiophen-2-yl)methylene) piperidin-4-one (3f): Dark Brown solid; Melting point: 112–114 °C: IR (KBr): 3034, 2991, 2348, 1804, 1714, 1509, 1365, 1012, 868, 742, 640 cm^{-1}: ^{1}H NMR (400 MHz, $CDCl_3$) δ ppm: 7.81 (d, J = 4.0 Hz, 2H), 7.62 (s, 1H), 7.21 (d, J = 4.0 Hz, 2H), 7.12 (s, 1H), 3.41 (d, J = 4.0 Hz, 4H), 2.37 (s, 6H), 2.22 (s, 3H); ^{13}C NMR (100 MHz, $CDCl_3$) δ ppm: 184.9, 146.7, 141.5, 140.4, 137.6, 137.1, 137.0, 130.6, 130.5, 129.9, 129.5, 128.6, 128.0, 62.6, 56.8, 45.2, 15.3, 15.2; HRMS for $C_{18}H_{19}NOS_2$ Calculated [M$^+$] m/z 329.4760, Found 329.4763.

(3Z,5E)-3,5-bis((5-hydroxythiophen-2-yl)methylene)-1-methylpiperidin-4-one (3g): Yellow solid; Melting point: 96–98 °C: IR (KBr): 3067, 2324, 1810, 1754, 1567, 1367, 1227, 787, 664, 642 cm^{-1}: ^{1}H NMR (400 MHz, $CDCl_3$) δ ppm: 9.72 (s, 2H), 8.42–8.41 (d, J = 4.0 Hz, 2H), 7.60 (s, 1H), 7.12 (s, 1H), 6.61 (d, J = 4.0 Hz, 2H), 3.40 (d, J = 4.0 Hz, 4H), 2.24 (s, 3H); ^{13}C NMR (100 MHz, $CDCl_3$) δ ppm: 185.9, 144.8, 142.0, 141.6, 140.0, 137.9, 137.8, 137.4, 131.8, 130.0, 129.8, 129.7, 129.0, 127.3, 127.0, 64.2, 56.4, 43.0; HRMS for $C_{16}H_{15}NO_3S_2$ Calculated [M$^+$] m/z 333.4200, Found 333.4203.

(3Z,5E)-3,5-bis((5-ethylthiophen-2-yl)methylene)-1-methylpiperidin-4-one (3h): Dark-Brown solid; Melting point: 116–118 °C: IR (KBr): 3028, 2367, 1787, 1569, 1345, 1247, 758, 684, 646 cm^{-1}: ^{1}H

NMR (400 MHz, $CDCl_3$) δ ppm: 7.77 (d, J = 8.0 Hz, 2H), 7.52 (s, 1H), 7.17 (d, J = 8.0 Hz, 2H), 7.14 (s, 1H), 3.31 (d, J = 4.0 Hz, 4H), 2.64–2.60 (m, 4H), 2.22 (s, 3H), 1.27 (t, J = 8.0 Hz, 6H); ^{13}C NMR (100 MHz, $CDCl_3$) δ ppm: 186.4, 146.7, 146.6, 142.2, 142.0, 141.9, 141.8, 141.7, 135.9, 135.7, 135.6, 126.9, 126.8, 64.0, 56.7, 44.9, 24.2, 24.1, 16.2, 16.1; HRMS for $C_{20}H_{23}NOS_2$ Calculated [M^+] m/z 357.5300, Found 357.5300.

(3Z,5E)-3,5-bis((4-bromo-5-methylthiophen-2-yl)methylene)-1-methylpiperidin-4-one (3i): Deep-Yellow solid; Melting point: 96–98 °C: IR (KBr): 2998, 2864, 1847, 1718, 1548, 1356, 1214, 864, 752, 644 cm^{-1}: ^{1}H NMR (400 MHz, $CDCl_3$) δ ppm: 7.74 (s, 2H), 7.56 (s, 1H), 7.08 (s, 1H), 3.31 (d, J = 8.0 Hz, 4H), 2.26 (s, 6H), 2.12 (s, 3H); ^{13}C NMR (100 MHz, $CDCl_3$) δ ppm: 186.2, 146.2, 141.9, 141.8, 138.4, 138.2, 138.0, 137.8, 137.6, 137.0, 123.2, 123.1, 110.2, 108.2, 108.1, 62.1, 55.9, 45.9, 15.2, 15.1; HRMS for $C_{18}H_{17}Br_2NOS_2$ Calculated [M^+] m/z 487.2680, Found 487.2679.

(3Z,5E)-1-methyl-3,5-bis((5-nitrothiophen-2-yl)methylene)piperidin-4-one (3j): Deep-Orange solid; Melting point: 112–114 °C: IR (KBr): 3064, 2994, 2224, 1846, 1756, 1504, 1421, 1202, 864, 752, 640 cm^{-1}: ^{1}H NMR (400 MHz, $CDCl_3$) δ ppm: 8.61 (d, J = 8.0 Hz, 2H), 7.81 (d, J = 8.0 Hz, 2H), 7.56 (s, 1H), 7.12 (s, 1H), 3.31 (d, J = 4.0 Hz, 4H), 2.28 (s, 3H); ^{13}C NMR (100 MHz, $CDCl_3$) δ ppm: 184.5, 146.1, 1417, 140.4, 137.6, 137.4, 137.0, 130.6, 130.5, 129.2, 129.0, 128.3, 128.1, 64.0, 56.4, 42.4; HRMS for $C_{16}H_{13}N_3O_5S_2$ Calculated [M^+] m/z 391.4160, Found 391.4163.

(3Z,5E)-1-methyl-3-((3-methylthiophen-2-yl)methylene)-5-((4-methylthiophen-2-yl)methyle ne)piperidin-4-one (3k): Orange solid; Melting point: 108–110 °C: IR (KBr): 3011, 2346, 1802, 1712, 1564, 1348, 1202, 752, 684, 640 cm^{-1}: ^{1}H NMR (400 MHz, $CDCl_3$) δ ppm: 8.02 (d, J = 4.0 Hz, 1H), 7.56 (s, 1H), 7.40 (d, J = 8.0 Hz, 1H), 7.26 (d, J = 8.0 Hz, 1H), 7.08 (s, 1H), 6.67 (d, J = 8.0 Hz, 1H), 3.17 (d, J = 4.0 Hz, 4H), 2.38 (s, 3H), 2.26 (d, J = 8.0 Hz, 6H); ^{13}C NMR (100 MHz, $CDCl_3$) δ ppm: 186.2, 152.4, 146.8, 146.7, 141.9, 141.8, 138.3, 137.9, 135.1, 131.9, 130.3, 127.7, 125.4, 62.1, 56.1, 45.0, 15.6, 14.5; HRMS for $C_{18}H_{19}NOS_2$ Calculated [M^+] m/z 329.4760, Found 329.4765.

(3Z,5E)-3,5-bis((4-fluoro-5-methylthiophen-2-yl)methylene)-1-methylpiperidin-4-one (3l): Brownish solid; Melting point: 120–122 °C: IR (KBr): 3120, 2998, 2214, 1864, 1702, 1564, 1312, 1212, 864, 752, 642 cm^{-1}: ^{1}H NMR (400 MHz, $CDCl_3$) δ ppm: 7.60 (s, 1H), 7.27 (d, J = 8.0 Hz, 2H), 7.12 (s, 1H), 3.21 (d, J = 4.0 Hz, 4H), 2.34 (s, 6H), 2.22 (s, 3H); ^{13}C NMR (100 MHz, $CDCl_3$) δ ppm: 184.1, 146.8, 141.9, 140.8, 137.8, 137.1, 137.0, 130.6, 130.5, 129.2, 129.1, 128.3, 128.0, 64.1, 56.8, 42.9; HRMS for $C_{18}H_{17}F_2NOS_2$ Calculated [M^+] m/z 365.4568, Found 365.4571.

2.2. Synthesis of (E)-5-methyl-2-phenyl-3-(thiophen-2-yl)-7-(thiophen-2-ylmethylene)-3,3a,4,5,6, 7-hexahydro-2H-pyrazolo[4,3-c]pyridine (5a-l)

A mixture of intermediate **3** (0.0025 mol) and phenylhydrazine (**4**) (0.0025 mol) was refluxed in 25 ml of isopropanol. The completion of reaction was monitored by TLC using ethyl acetate and hexane mixture (1:9) as eluent. Once the reaction completed, the reaction mixture was kept aside to reach room temperature and poured into the crushed ice with continuous stirring and the solid obtained was filtered and washed with water. The crude product was dried and purified over column chromatography using ethyl acetate and hexane (1:9) as an eluen. The isolated pure and final product from column chromatography was recrystallized using ethanol and THF in 1:1 ratio.

(E)-5-methyl-2-phenyl-3-(thiophen-2-yl)-7-(thiophen-2-ylmethylene)-3,3a,4,5,6,7-hexahydro-2H-pyrazolo [4,3-*c*] pyridine (5a): Pale yellow powder; Melting point: 168–170 °C: IR (KBr): 3096, 3022, 2916, 2870, 2334, 1732, 1584, 1462, 1432, 1386, 1260, 1212, 1116, 897, 756, 694, 672, 666, 642 cm^{-1}: ^{1}H NMR (400 MHz, $CDCl_3$) δ ppm: 8.13 (s, 1H), 8.06 (d, J = 8.0 Hz, 1H), 7.91–7.90 (m, 2H), 7.48–7.16 (m, 8H), 3.96 (d, J = 3.6 Hz, 2H), 3.72–3.64 (m, 2H), 2.83–2.69 (m, 2H), 2.27 (s, 3H); ^{13}C NMR (100 MHz, $CDCl_3$) δ ppm: 164.5, 164.4, 162.1, 162.0, 156.0, 147.2, 147.1, 146.6, 145.7, 145.6, 137.9, 130.4, 130.3, 129.9, 129.8, 129.3, 129.2, 126.2, 126.0, 122.4, 122.3, 122.2, 122.1, 116.9, 114.5, 114.3, 60.1, 57.8, 55.1, 33.7, 31.1; Elemental Analysis, Calculated: C, 67.49; H, 5.41; N, 10.73; S, 16.38; Obtained: C, 67.51; H, 5.43; N, 10.71; S, 16.36; HRMS for $C_{22}H_{21}N_3S_2$ Calculated [M^+] m/z 391.5510, Found 391.5510.

(E)-5-methyl-2-phenyl-3-(thiophen-3-yl)-7-(thiophen-3-ylmethylene)-3,3a,4,5,6,7-hexahydro-2H-pyrazolo [4,3-*c*] pyridine (5b): Light-Orange solid; Melting point: 178–180 °C: IR (KBr): 3108, 3024, 2934, 2858, 2306, 1742, 1590, 1468, 1406, 1380, 1268, 1234, 1112, 898, 760, 698, 678, 662 cm^{-1}: ^{1}H NMR (400 MHz, $CDCl_3$) δ ppm: 8.07–7.81 (m, 6H), 7.50–7.37 (m, 5H), 7.06 (s, 1H), 4.54 (d, J = 8.0 Hz, 1H), 3.59–3.56 (m, 2H), 2.87–2.65, (m, 3H), 2.30–2.28 (m, 3H); ^{13}C NMR (100 MHz, $CDCl_3$) δ ppm: 156.1, 147.1, 144.1, 142.7, 138.0, 137.9, 137.8, 128.8, 128.7, 128.4, 127.9, 127.8, 127.3, 126.9, 126.0, 125.6, 123.6, 123.6, 115.9, 33.6, 30.9; Elemental Analysis, calculated: C, 67.49; H, 5.41; N, 10.73; S, 16.38; Obtained: C, 67.48; H, 5.43; N, 10.72; S, 16.40; HRMS for $C_{22}H_{21}N_3S_2$ Calculated [M^+] m/z 391.5510, Found 391.5510.

(E)-3-(5-bromothiophen-2-yl)-7-((5-bromothiophen-2-yl)methylene)-5-methyl-2-phenyl-3, 3a,4,5,6,7-hexahydro-2H-pyrazolo [4,3-*c*] pyridine (5c): Pale yellow powder; Melting point: 190–192 °C: IR (KBr): 3024, 3012, 2924, 2858, 2345, 1818, 1748, 1564, 1432, 1378, 1268, 1234, 1112, 896, 760, 698, 676, 662, 640 cm^{-1}: ^{1}H NMR (400 MHz, $CDCl_3$) δ ppm: 7.74–7.32 (m, 2H), 7.27–7.15 (m, 6H), 6.87 (d, J = 4.0 Hz, 1H), 3.73 (d, J = 4.0 Hz, 2H), 3.59–3.40 (m, 2H), 2.80–2.70 (m, 2H), 2.31–2.01 (m, 4H); ^{13}C NMR (100 MHz, $CDCl_3$) δ ppm: 160.5, 143.4, 142.5, 141.1, 139.5, 138.1, 137.2, 132.9, 130.9, 129.9, 129.8, 128.4, 127.6, 127.5, 127.1, 126.9, 126.3, 124.5, 122.5, 119.4, 116.6, 110.2, 96.4, 60.2, 59.3, 52.7, 43.8, 43.6; Elemental Analysis, calculated: C, 48.10; H, 3.49; Br, 29.09; N, 7.65; S, 11.67; Obtained: C, 48.12; H, 3.47; Br, 29.11; N, 7.63; S, 11.67; HRMS for $C_{22}H_{19}Br_2N_3S_2$ Calculated [M^+] m/z 549.3430, Found 549.3432.

(E)-3-(5-chlorothiophen-2-yl)-7-((5-chlorothiophen-2-yl)methylene)-5-methyl-2-phenyl-3,3a,4,5,6,7-hexahydro-2H-pyrazolo [4,3-*c*] pyridine (5d): Pale yellow powder; Melting point: 194–196 °C: IR (KBr): 3024, 2996, 2884, 2320, 1738, 1588, 1470, 1436, 1348, 1234, 1208, 1120, 888, 768, 670, 662, 656, 642 cm^{-1}: ^{1}H NMR (400 MHz, $CDCl_3$) δ ppm: 7.15–6.96 (m, 5H), 6.47–6.31 (m, 2H), 6.24–6.17 (m, 2H), 3.95 (d, J = 8.0 Hz, 1H), 3.53–3.42 (m, 2H), 2.86–2.70 (m, 2H), 2.41–2.11 (m, 5H); ^{13}C NMR (100 MHz, $CDCl_3$) δ ppm: 156.4, 147.3, 144.4, 142.9, 138.3, 138.2, 138.0, 126.2, 125.9, 123.8, 123.8, 116.1, 113.2, 59.8, 58.4, 55.4, 33.8, 31.1; Elemental Analysis, calculated: C, 57.39; H, 4.16; Cl, 15.40; N, 9.13; S, 13.93; Obtained: C, 57.37; H, 4.18; Cl, 15.42; N, 9.11; S, 13.95; HRMS for $C_{22}H_{19}Cl_2N_3S_2$ Calculated [M^+] m/z 460.4350, Found 460.4350.

(E)-3-(5-fluorothiophen-2-yl)-7-((5-fluorothiophen-2-yl)methylene)-5-methyl-2-phenyl-3,3a,4,5,6,7-hexahydro-2H-pyrazolo [4,3-*c*] pyridine (5e): Yellowish solid; Melting point: 186–188 °C: IR (KBr): 3088, 3021, 2918, 2866, 2331, 1734, 1586, 1464, 1432, 1387, 1265, 1213, 1118, 894, 754, 696, 674, 664, 641 cm^{-1}: ^{1}H NMR (400 MHz, $CDCl_3$) δ ppm: 7.24 (d, J = 2.8 Hz, 2H), 7.14–7.06 (m, 5H), 6.96–6.88 (m, 1H), 6.69–6.63 (m, 1H), 6.57–6.37 (m, 1H), 3.74 (d, J = 4.0 Hz, 1H), 2.85–2.75 (m, 2H), 2.17–2.10 (m, 2H), 1.56–1.45 (m, 4H); ^{13}C NMR (100 MHz, $CDCl_3$) δ ppm: 164.6, 164.5, 162.1, 162.0, 156.0, 147.1, 147.0, 146.7, 145.8, 145.7, 137.9, 130.5, 130.4, 130.0, 129.9, 129.3, 122.2, 122.1, 117.1, 114.5, 113.8, 113.2, 97.8, 60.18, 57.8, 33.7, 31.2; Elemental Analysis calculated: C, 61.81; H, 4.48; F, 8.89; N, 9.83; S, 15.00; Obtained: C, 61.83; H, 4.46; F, 8.89; N, 9.81; S, 15.02; S, 9.13; HRMS for $C_{22}H_{19}F_2N_3S_2$ Calculated [M^+] m/z 427.5318, Found 427.5317.

(E)-5-methyl-3-(5-methylthiophen-2-yl)-7-((5-methylthiophen-2-yl)methylene)-2-phenyl-3, 3a,4,5,6,7-hexahydro-2H-pyrazolo [4,3-*c*] pyridine (5f): Light-brown powder; Melting point: 182–184 °C: IR (KBr): 3084, 3016, 2977, 2836, 2334, 1750, 8 1464, 1434, 1386,

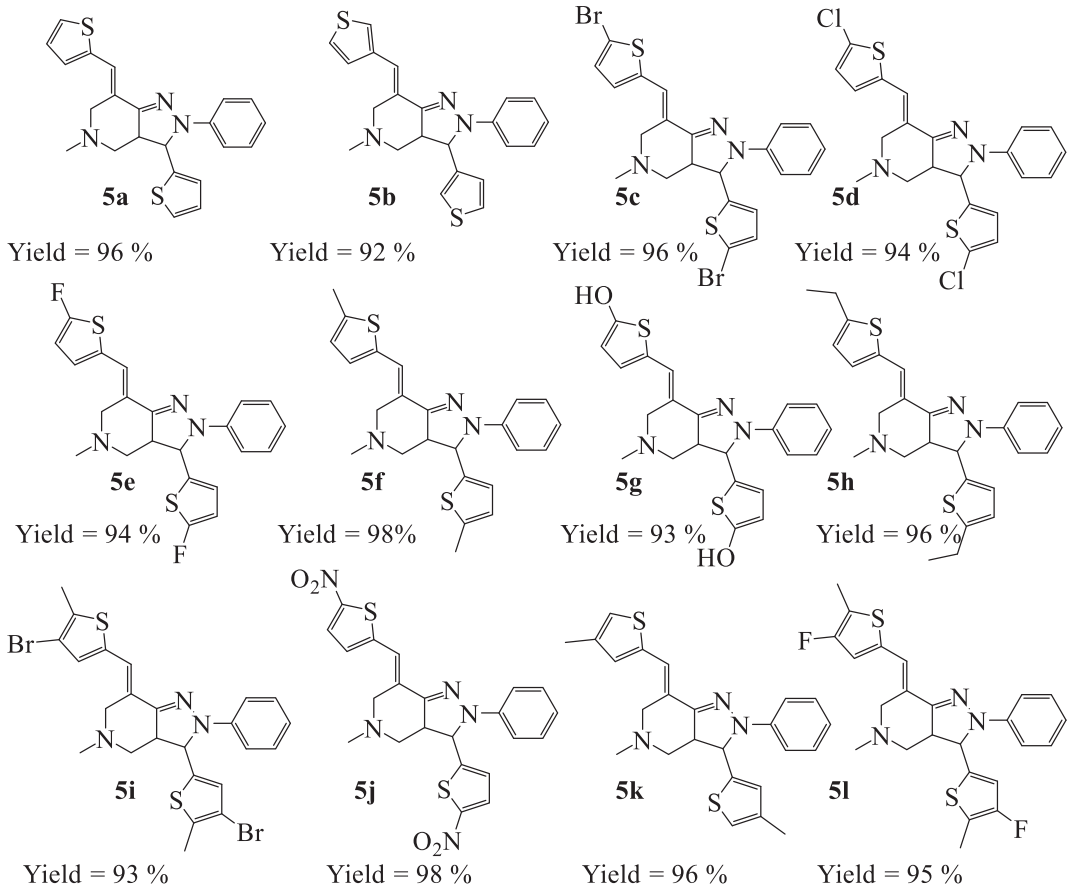

Fig. 2. The achieved and final structures of targeted pyrazolopyridines (**5a-l**).

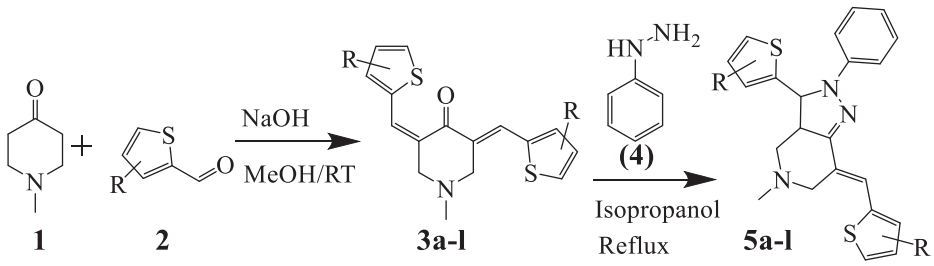

Scheme 1. Route of synthesis of intermediates (3Z,5E)-1-methyl-3,5-bis(thiophen-2-ylmethylene) piperidin-4-one derivatives (**3a-l**) and pyrazolopyridines (**5a-l**).

Table 1
Molecular mechanistic values of pyrazolopyridine (**5a-l**) molecular docking results.*

Entity	Binding energy	Ligand efficiency	Inhibitory constant (*ki*) (nM)
5a	−12.45	−0.46	1.02
5b	−11.97	−0.42	2.45
5c	−10.14	−0.41	4.28
5d	−9.48	−0.36	6.32
5e	−9.18	−0.35	8.17
5f	−9.94	−0.38	4.02
5g	−14.13	−0.48	0.58
5h	−10.97	−0.43	2.84
5i	−11.14	−0.44	2.08
5j	−13.48	−0.46	0.92
5k	−10.08	−0.39	2.74
5l	−10.35	−0.41	2.18

* 1CX2 (PDB crystal structure of COX-2).

1264, 1234, 1112, 892, 758, 694, 676, 648 cm^{-1}: ^1H NMR (400 MHz, $CDCl_3$) δ ppm: 7.86 (t, J = 8.0 Hz, 2H), 7.64 (d, J = 2.0 Hz, 2H), 7.32–6.80 (m, 1H), 6.78–6.69 (m, 5H), 6.52 (d, J = 8.0 Hz, 1H), 3.92 (d, J = 3.2 Hz, 2H), 3.05–3.00 (m, 2H), 2.98 (d, J = 8.0 Hz, 1H), 2.82–2.18 (m, 9H); ^{13}C NMR (100 MHz, $CDCl_3$) δ ppm: 160.6, 143.4, 142.6, 141.3, 139.5, 138.2, 137.3, 132.9, 130.9, 130.0, 129.8, 128.4, 127.7, 127.4, 127.1, 126.9, 126.4, 125.5, 124.6, 122.5, 119.5, 116.7, 60.3, 59.3, 43.9, 43.6, 13.8, 12.4; Elemental Analysis, calculated: C, 68.70; H, 6.01; N, 10.01; S, 15.28; Obtained: C, 68.70; H, 6.03; N, 10.02; S, 15.25; HRMS for $C_{24}H_{25}N_3S_2$ Calculated $[M^+]$ m/z 419.6050, Found 419.6050.

(E)-5-((3-(5-hydroxythiophen-2-yl)-5-methyl-2-phenyl-2,3,3a,4,5,6-hexahydro-7H-pyrazolo [4,3-c] pyridin-7-ylidene)methyl)thiophen-2-ol (5g): Pale yellow solid; Melting point: 178–180 °C: IR (KBr): 3064, 3014, 2964, 2828, 2345, 1738, 1576, 1420, 1408, 1388, 1234, 1212, 892, 696, 662 cm^{-1}: ^1H NMR (400 MHz, $CDCl_3$) δ ppm: 11.62 (s, 2H), 8.13 (s, 1H), 8.06 (d, J = 8.0 Hz, 1H), 7.97–7.90 (m, 2H), 7.46 (t, J = 8.0 Hz, 1H), 7.39 (d, J = 8.0 Hz, 3H), 7.18 (d,

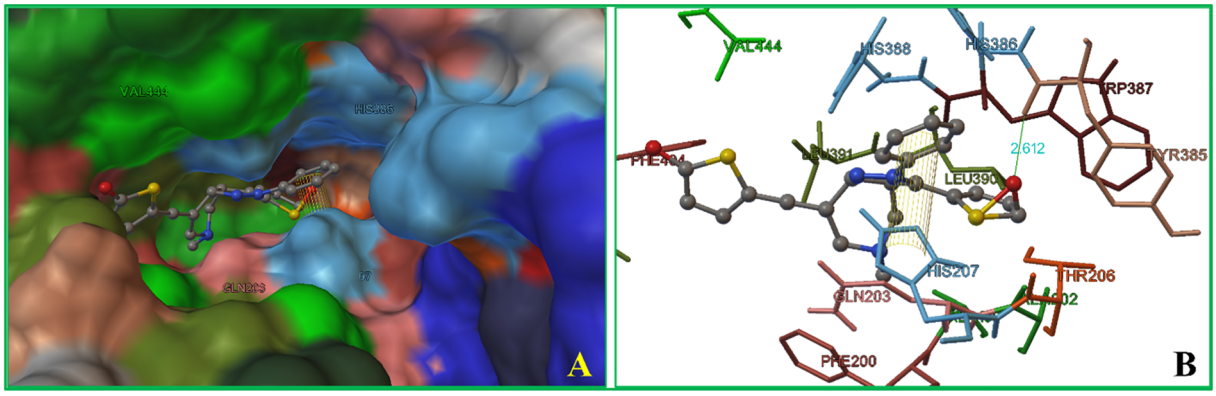

Fig. 3. Molecular interaction results of compound **5g** to COX-2.

Table 2
Druggability score prediction results of pyrazolopyridines (**5a-l**).

Name	DiffCoef	MlogP	S+logP	S+logD	RuleOf5	RuleOf5_Code	MWt	M_NO
5a	0.660	3.947	4.118	3.701	0	<None>	391.56	3
5b	0.660	3.947	3.816	3.535	0	<None>	391.56	3
5c	0.616	5.116	5.587	5.325	2	Mw; LP	549.362	3
5d	0.627	4.909	5.583	5.355	1	LP	460.45	3
5e	0.653	4.698	5.202	4.928	1	LP	427.541	3
5f	0.621	4.373	5.098	4.794	1	LP	419.614	3
5g	0.646	2.887	3.502	3.227	0	<None>	423.558	5
5h	0.588	4.785	5.916	5.674	1	LP	447.668	3
5i	0.583	5.522	6.348	6.155	2	Mw; LP	577.416	3
5j	0.621	4.065	4.403	4.312	0	<None>	481.555	9
5k	0.621	4.373	5.104	4.801	1	LP	419.614	3
5l	0.616	5.116	5.828	5.616	1	LP	455.595	3

Notes: MlogP. Moriguchi estimation of logP. HBDH. A number of Hydrogen bond donor protons. M_NO. A total number of Nitrogen and Oxygen atoms. T_PSA. The topological polar surface area in square angstroms. Ro5 - Rule Of Five. Rule Of Five_Code; Mw = molecular weight; NO = number of Nitrogen- and Oxygen-based Hydrogen bond acceptors.

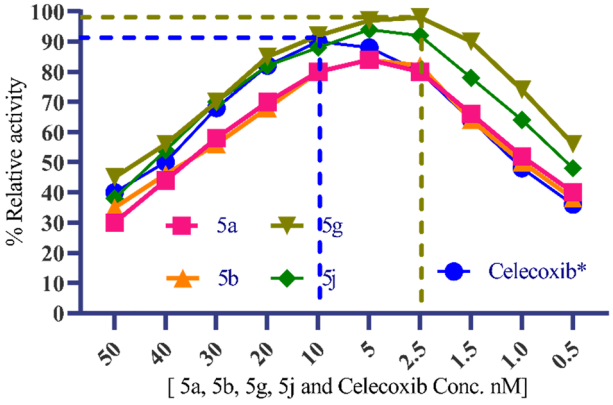

Fig. 4. Dose-response curve cum relative percentage activity results of COX-2 inhibition activity of pyrazolopyridines **5a**, **5b**, **5g,** and **5j.**

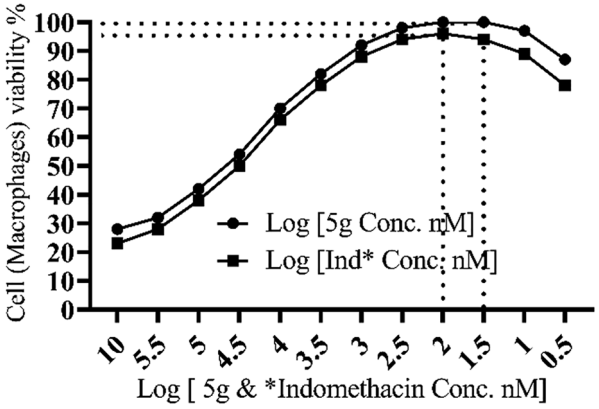

Fig. 5. Cell viability in macrophages treated with **5g** and Indomethacin at 1 to 10 (nM), as assessed by the MTT assay. Results are expressed as the % of living cells comparative to control cells. The results are the mean of three repeated assay values.

J = 2.0 Hz, 1H), 7.16 (s, 1H), 3.96 (d, J = 4.0 Hz, 1H), 3.72–3.64 (m, 2H), 2.83–2.69 (m, 2H), 2.27–2.13 (m, 4H); ^{13}C NMR (100 MHz, $CDCl_3$) δ ppm: 156.5, 147.5, 144.5, 143.1, 138.4, 138.3, 138.2, 129.2, 129.1, 128.8, 128.3, 128.2, 127.7, 127.4, 127.3, 126.4, 126.0, 124.0, 124.0, 116.3, 113.3, 59.9, 58.6, 33.9, 31.1; Elemental Analysis, calculated: C, 62.39; H, 5.00; N, 9.92; O, 7.55; S, 15.14; Obtained: C, 62.37; H, 5.02; N, 9.94; O, 7.55; S, 15.12; HRMS for $C_{22}H_{21}N_3O_2S_2$ Calculated $[M^+]$ m/z 423.5490, Found 423.5491.

(E)-5-((3-(5-hydroxythiophen-2-yl)-5-methyl-2-phenyl-2,3,3a,4,5,6-hexahydro-7H-pyrazolo [4,3-c] pyridin-7-ylidene) methyl)thiophen-2-ol (5h): Yellow solid; Melting point: 164–166 °C: IR (KBr): 3024, 2978, 2864, 2364, 1774, 20 1548, 1424, 1325, 1264, 1234, 1024, 868, 656, 678, 642 cm^{-1}: ^{1}H NMR (400 MHz, $CDCl_3$) δ ppm: 7.95–7.77 (m, 6H), 7.45–7.26 (m, 4H), 4.43 (d, J = 4.0 Hz, 1H), 3.30 (t, J = 8.0 Hz, 2H), 2.76–2.70 (m, 4H), 2.57–2.49 (m, 2H), 2.19–2.06 (m, 4H), 1.50 (t, J = 8.0 Hz, 6H); ^{13}C NMR (100 MHz, $CDCl_3$) δ ppm: 156.3, 147.3, 144.3, 138.2, 138.1, 138.0, 129.0, 128.9, 128.6, 128.1, 128.0, 127.5, 127.2, 127.1, 126.2, 125.8, 123.8, 123.8,

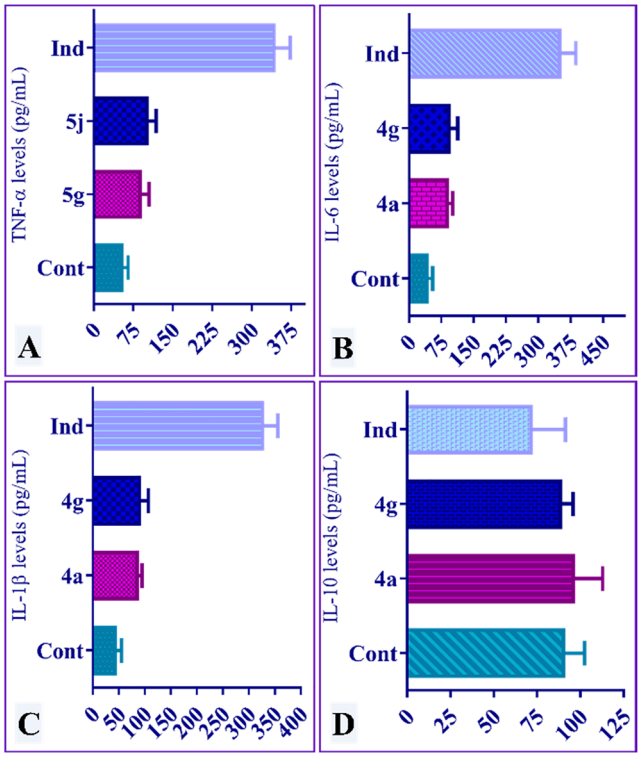

Fig. 6. Effects of pyrazolopyridines **5g**, **5j** and Indomethacin on the LPS-stimulated levels of (A) TNF-α, (B) IL-1β, (C) IL-6 and (D) IL-10 levels in macrophages. The concentrations were assessed and finalized by ELISA. The results are the mean of three determinations ± SEM.

116.8, 59.7, 58.4, 55.3, 33.7, 31.1, 21.9, 21.7, 15.0; Elemental Analysis, calculated: C, 69.76; H, 6.53; N, 9.39; S, 14.32; Obtained: C, 69.74; H, 6.55; N, 9.37; S, 14.34; HRMS for $C_{26}H_{29}N_3S_2$ Calculated $[M^+]$ *m/z* 447.6590, Found 447.6595.

(E)-3-(5-ethylthiophen-2-yl)-7-((5-ethylthiophen-2-yl)methylene)-5-methyl-2-phenyl-3,3a, 4,5,6,7-hexahydro-2H-pyrazolo [4,3-*c*] pyridine (5i): Yellow solid; Melting point: 220–222 °C: IR (KBr): 3012, 3008, 2998, 2902, 2871, 2345, 1787, 1504, 1470, 1412, 1340, 1266, 1234, 1109, 878, 672, 642 cm^{-1}: ^1H NMR (400 MHz, $CDCl_3$) δ ppm: 7.01 (d, J = 8.0 Hz, 2H), 6.98–6.90 (m, 1H), 6.88–6.77 (m, 1H), 6.45–6.35 (m, 3H), 6.24 (s, 1H), 3.53 (d, J = 4.0 Hz, 1H), 2.74–2.60 (m, 4H), 2.59–2.15 (m, 10*H*); ^{13}C NMR (100 MHz, $CDCl_3$) δ ppm: 156.2, 147.1, 144.2, 142.8, 138.1, 138.0, 137.8, 128.8, 128.7, 128.5, 128.0, 127.9, 127.3, 127.1, 127.0, 126.0, 125.7, 123.7, 123.6, 116.0, 113.0, 59.6, 58.3, 55.2, 33.6, 31.0, 21.8, 21.6, 14.9; Elemental Analysis, calculated: C, 49.92; H, 4.02; Br, 27.68; N, 7.28; S, 11.11; Obtained: C, 49.94; H, 4.00; Br, 27.68; N, 7.30; S, 11.09; HRMS for $C_{24}H_{23}Br_2N_3S_2$ Calculated $[M^+]$ *m/z* 577.3970, Found 577.3970.

(E)-5-methyl-3-(5-nitrothiophen-2-yl)-7-((5-nitrothiophen-2-yl) methylene)-2-phenyl-3,3a,4, 5,6,7-hexahydro-2H-pyrazolo [4,3-*c*] pyridine (5j): Pale orange solid; Melting point: 196–198 °C: IR (KBr): 3098, 3012, 2981, 2862, 2345, 1742, 1562, 1464, 1432, 1340, 1245, 1234, 1148, 890, 668, 642 cm^{-1}: ^1H NMR (400 MHz, $CDCl_3$) δ ppm: 8.38 (d, J = 8.0 Hz, 1H), 8.06 (d, J = 8.0 Hz, 1H), 7.93–7.86 (m, 3H), 7.43–7.36 (m, 2H), 7.07–7.04 (m, 3H), 3.93 (d, J = 4.0 Hz, 1H), 3.01 (t, J = 8.0 Hz, 2H), 2.68–2.63 (m, 2H), 2.41–2.11 (m, 4H); ^{13}C NMR (100 MHz, $CDCl_3$) δ ppm: 168.4, 156.3, 147.2, 143.3, 142.1, 141.3, 140.3, 138.1, 129.0, 128.9, 128.2, 127.8, 126.7, 126.4, 26.0, 125.7, 116.0, 113.0, 59.7, 58.2, 54.9, 47.0, 42.1, 42.1; Elemental Analysis, calculated: C, 54.87; H, 3.98; N, 14.54; O, 13.29; S, 13.32; Obtained: C, 54.89; H, 3.96; N, 13.30; S, 13.31; HRMS for $C_{22}H_{19}N_5O_4S_2$ Calculated $[M^+]$ *m/z* 481.5450, Found 481.5450.

(E)-5-methyl-3-(4-methylthiophen-2-yl)-7-((4-methylthiophen-2-yl)methylene)-2-phenyl-3, 3a,4,5,6,7-hexahydro-2H-pyrazolo [4,3-*c*] pyridine (5k): Pale orange-solid; Melting point: 184–186 °C: IR (KBr): 3085, 3008, 2925, 2865, 2324, 1736, 1547, 1424, 1443, 1312, 1234, 1210, 1120, 886, 858, 792, 686, 664, 642 cm^{-1}: ^1H NMR (400 MHz, $CDCl_3$) δ ppm: 7.22 (d, J = 4.0, 3H), 7.06–7.01 (m, 1H), 6.83–6.77 (m, 1H), 6.68 (d, J = 8.0 Hz, 1H), 6.57 (d, J = 8.0 Hz, 2H), 6.43 (d, J = 8.0 Hz, 1H), 6.26 (d, J = 8.0 Hz, 1H), 3.78 (d, J = 4.0 Hz, 1H), 3.01–2.97 (m, 2H), 2.87–2.83 (m, 2H), 2.41–2.17 (m, 10*H*); ^{13}C NMR (100 MHz, $CDCl_3$) δ ppm: 169.3, 157.6, 156.2, 155.1, 147.0, 138.7, 126.0, 125.2, 120.8, 119.8, 115.9, 55.6, 55.0, 53.4, 53.3, 51.0, 15.4, 15.0; Elemental Analysis, calculated: C, 68.70; H, 6.01; N, 10.01; S, 15.28; Obtained: C, 68.72; H, 6.01; N, 10.03; S, 15.26; HRMS for $C_{24}H_{25}N_3S_2$ Calculated $[M^+]$ *m/z* 419.6050, Found 419.6050.

(E)-3-(4-fluoro-5-methylthiophen-2-yl)-7-((4-fluoro-5-methylthiophen-2-yl)methylene)-5-methyl-2-phenyl-3,3a,4,5,6,7-hexahydro-2H-pyrazolo [4,3-*c*] pyridine (5l): Light-Brownish solid; Melting point: 198–200 °C: IR (KBr): 3186, 3002, 2980, 2890, 2345, 1766, 1539, 1426, 1424, 1340, 1234, 1212, 1108, 896, 758, 696, 672, 662, 648 cm^{-1}: ^1H NMR (400 MHz, $CDCl_3$) δ ppm: 7.02–6.90 (m, 2H), 6.88–6.77 (m, 1H), 6.45–6.41 (m, 4H), 6.37–6.24 (m, 1H), 3.80 (s, 1H), 3.32 (s, 2H), 2.74–2.56 (m, 2H), 2.15–2.12 (m, 10*H*); ^{13}C NMR (100 MHz, $CDCl_3$) δ ppm: 156.0, 147.2, 144.1, 142.8, 138.1, 138.0, 128.8, 128.7, 128.1, 128.0, 127.9, 127.3, 127.1, 127.0, 126.0, 125.7, 123.7, 123.6, 116.0, 113.0, 59.6, 56.3, 55.0, 33.6, 31.1, 21.8, 21.1, 14.9; Elemental Analysis, calculated: C, 63.27; H, 5.09; F, 8.34; N, 9.22; S, 14.07; Obtained: C, 63.27; H, 5.08; F, 8.35; N, 9.20; S, 14.09; HRMS for $C_{24}H_{23}F_2N_3S_2$ Calculated $[M^+]$ *m/z* 455.5858, Found 455.5856.

2.3. *In silico molecular docking studies*

In silico molecular docking studies of pyrazolopyridine (**5a-l**) was carried out using Autodock4.2.6, AutoDock Tools 1.5.6, ChemDraw 15.0 and Arguslab 4.0.1. All parameters were performed according to

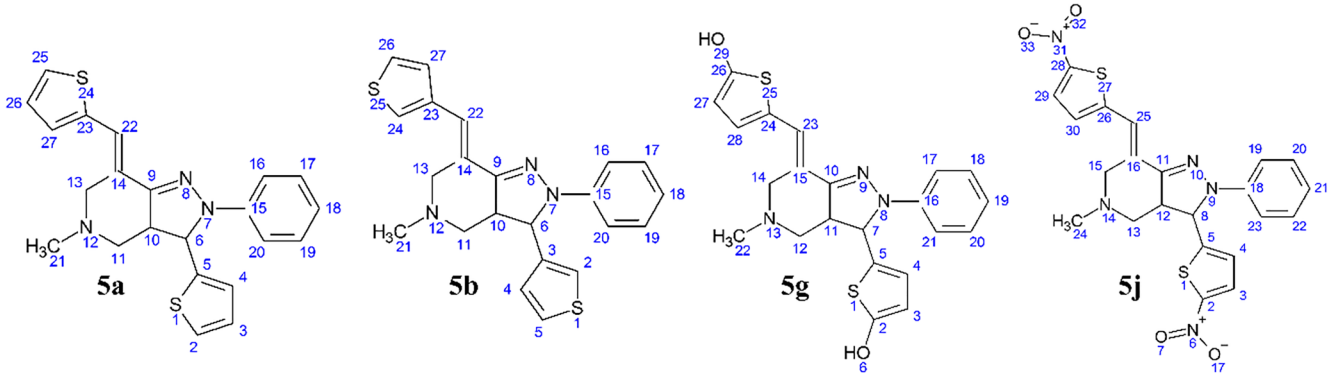

Fig. 7. Fuctional group substitution specifics of pyrazolopyridines **5a**, **5b**, **5g**, and **5j**.

our previous reports [20–22]. 3D crystal structure of COX-2 (PDB ID: 1CX2) downloaded from www.rcsb.org/pdb/. The ligand structure of **5a-l** was docked into the active binding-sites of COX-2 (1CX2). The obtained statistical mechanistic values for the target compounds such as lowest binding energy, ligand efficiency, and the inhibitory constant (*ki*) values were assessed for internal-compounds standard among **5a-l** in order to screen them for further target biological activity.

2.4. In vitro COX-2 inhibition studies

The assay was conducted using the commercially available COX-2 inhibitor screening kit (K547-100-BioVision, USA) [23,24]. Apart from pyrazolopyridine (**5a-l**), the assay mixture had prescribed amounts of EDTA (3 mM), Tris–HCl buffer (100 mM, pH 8.0), haematin (15 mM), and COX-2 enzyme. Arachidonic acid and N,N,N′,N′-tetramethyl-p-phenylenediamine (TMPD) were added together to make the total volume to 1 ml. The assay mixture was pre-incubated at 22 °C for 1 min along with the test compounds. As the activity measurement, the rate of TMPD oxidation in 20 s was read at 602 nm absorbance.

2.5. In vitro anti-inflammatory assessment of pyrazolopyridine (5a-l)

Human Red Blood Cell (HRBC) membrane stabilization based anti-inflammatory study was conducted to confirm the constancy of HRBC membrane, which is supposed to inhibit the inflammatory progression by limiting the discharge of lysosomal enzymes by pyrazolopyridine (**5a-l**). The proposed activity was carried out (n = 4) using indomethacin as standard [25,26]. The percentage of hemolysis was calculated by assuming the hemolysis produced in the presence of distilled water at 100%. The percentage of HRBC membrane stabilization was calculated using the following formula,

$$\%\ \text{inhibition of hemolysis} = 100 \times [(OD_1 - OD_2)/OD_1]$$

where OD_2 = optical density of sample OD_1 = optical density of control.

2.6. Cell viability assay using macrophages

Commercially obtained macrophages (J774A.1) was used to assess the cell viability after treating pyrazolopyridine (**5a-l**). Macrophage cells were washed with a PBS buffer prior to use it for sub-culturing and subsequent cytotoxicity assessments [27]. After decanting PBS buffer, the cells were seeded in Dulbecco's Modified Eagle's Medium (DMEM) at a density of 8×10^4 cells per well (96-well microtiter plates) and incubated for 24 h in a 5% CO_2 atmosphere. The selected pyrazolopyridines among **5a-l** were dissolved in DMSO at a concentration of 10^{-1} to 10^{-8} (μg/mL). These concentrations were treated up to 48 h and then 10 μL (10 mg/mL in a PBS buffer) of MTT (3-(4,5-dimethylthiazol-2-yl)-2,5-diphenyl tetrazolium bromide) was added and incubated for 6–8 h at 37 °C. The Formazan crystals formed due to the reaction were dissolved in 100 μL of DMSO after taking out the DMEM from corresponding wells of the microtiter plates. The optical density (OD) was resolute at 540 nm in BioRad ELISA plate reader.

$$\text{Mean OD treatment/mean OD control} \times 100 = \_\%$$

2.7. The assessment of pro- & anti-inflammatory interleukin levels in LPS induced macrophages

In order to assess the pro- & anti-inflammatory interleukin levels in J77A,1 macrophage, TNF-α, IL-1β, IL-6, and IL-10 serum levels were measured by ELISA method. Macrophages were sub-cultured with a density of 1×10^6 in DMEM. Further, pyrazolopyridine (**5a-l**) and Indomethacin (0.5 to 50 nM) were treated in different concentration range (1 mg/mL) by incubating the cells for 120 min. Lipopolysaccharides (LPS) was added to the cells at 1 μg/mL range and incubated for 24 h and further, the cell-free supernatants were obtained and analyzed by means of immunoassay and the cytokines level was quantified. The concentrations of TNF-α, IL-1β, IL-6, and IL-10 and in the supernatants of macrophages confirmed by means of immune-enzymatic assessments.

2.8. Statistical analysis

All the obtained results were statistically analyzed through one-way ANOVA with Dunnett's post-test. GraphPad Prism version 8.0 software was used for analysis. The results are stated as mean ± SEM and a difference was considered statistically significant if $p \leq 0.05$.

3. Results and discussions

3.1. Synthesis of target compounds pyrazolopyridines (5a-l)

The synthesis of target compounds pyrazolopyridines (**5a-l**) given in Fig. 2 was accomplished by a two-step reaction process as outlined in Scheme 1. The intermediate (3Z,5E)-1-methyl-3,5-bis(thiophen-2-ylmethylene)piperidin-4-one derivatives (**3**) synthesized according to the reported procedure by Liang et al. [28]. Conversion of (**1** + **2**) into **3a-l** was achieved by using 1 mol of 1-methylpiperidin-4-one, 2 mol of substituted thiophene-carbaldehydes in presence of 15 ml of methanol under stirring conditions, followed by dropwise addition of NaOH (5 mol %). Reaction between phenylhydrazine (**4**) and intermediate (3Z,5E)-1-methyl-3,5-bis(thiophen-2-ylmethylene)piperidin-4-one derivatives (**3a-l**) afforded pyrazolopyridines (**5a-l**) in excellent yields (92–98%).

3.2. Results of in silico druggability and molecular docking studies

As depicted in Table 1, the overall molecular docking results ensured the capability of, almost all pyrazolopyridines (**5a-l**), inhibition potential of COX-2. Because, the average least binding energy (−11.11 kcal/mol), ligand efficiency (−0.42) and binding affinity (3.14 nM) were excellent. Based on these molecular mechanistic values, the individual best compounds **5a**, **5b**, **5g,** and **5j** were screened for further *in vitro* and *in vivo* anti-inflammatory assessments. Fig. 3 illustrates the mode of molecular interaction *in silico* between COX-2 and the best compound **5g**. Compound **5g** found to have both hydrogen bonding (Tyr385; bond angle 2.6 Å) and a π-π interaction (non-covalent) between His207 & aryl ring 2. This interaction should have facilitated the firm COX-2 inhibition possessed by the representative compounds **5g** among **5a-l**. From which, the COX-2 inhibition plausible mechanism would be understood.

A structure-based druggability assessment was carried-out for pyrazolopyridines (**5a-l**) using different stand-alone (MedChem Designer 5.0) and online tools (pkCSM). The obtained results of three repeated predictions averaged and tabulated for considerations (Table 2). MlogP - Moriguchi estimation of logP (a measure of the difference in solubility of the compound in these two phases) was not a problem against the potentially identified compounds **5a**, **5b**, **5g** and **5j** (Table 2 – highlighted in green). A total number of Nitrogen and Oxygen atoms was minimum 3 and maximum 9 ensured the crucial electron donation and acceptation between the range of amino acid residues and these compounds. Rule of Five_Code (Ro5 code) found to be 'zero' means, these compounds have no violations and adopting to Lipinski's five rule [29].

3.3. Results of in vitro COX-2 inhibition studies

Potentially identified COX-2 inhibitors **5a**, **5b**, **5g** and **5j** from molecular docking studies were only used to assess their COX-2 inhibition ability *in vitro*. N,N,N,N-tetramethyl-p-phenylenediamine (TMPD) oxidation based chromogenic assay during the reduction of Prostaglandin G2 (PGG2) to Prostaglandin H2 (PGH2) was employed [23,24]. In the

activity assessments, we found a dose of depended on inhibitory activity from all these compounds. As the molecular docking studies indicated, pyrazolopyridines (**5a**, **5b**, **5g,** and **5j**) were testified in the different concentration range of 0.5–50 nM.

In the activity, the compounds did inhibit COX-2 in 2–10 nM up to 98%. There was no activity or only a lesser activity found in concentration ranges 0.5–1.5 nM and 15–50 nM. The same condition was also applicable for the standard drug Celecoxib. Fig. 4 illustrates the dose depended COX-2 activity showed by pyrazolopyridines **5a**, **5b**, **5g,** and **5j.** Compound stability was good for **5g** and **5j** as they showed a steady COX-2 inhibition in 2–5 nM concentrations. The IC_{50} required for **5g** and **5j** was 2.25 ± 0.02 nM to have an average relative percentage activity of 96.25 ± 1.99. This was quite interesting while comparing the IC_{50} (10.25 ± 0.75 nM) and relative % activity (90.25 ± 2.65) of Celecoxib, the standard COX-2 inhibitor. Thus, **5g** and **5j** screened for further *in vitro* and *in vivo* anti-inflammatory activity in HRBC and macrophages respectively.

3.4. Results of in vitro anti-inflammatory activity

The inhibition capability of discharge of lysosomal enzymes in HRBC was taken as a measure to adjudge the anti-inflammatory effect **5g** and **5j**. Relative percentage activity (RPA) and IC_{50} values were taken in account to determine the activities among **5g** and **5j** by comparing the values obtained for the standard drug (Diclofenac) (RPA = 89.25 ± 2.45 & IC_{50} 1.15 μM). An increased lysosomal ingredient discharge arrest from HRBC was found in 0.012 ± 0.002 μM (IC_{50} 0.006 μM) from a tested concentration range of 0.01–0.25 μM. Serially diluted (initial volume of 0.01 μM in 100 μL) concentrations of the target compounds were assessed in four repeated assays. In the overall results, compounds **5g** and **5j** were showed most valuable results (RPA = 96.25 ± 2.15 & IC_{50} 0.006 ± 0.001 μM and RPA = 91.75 ± 2.24 & IC_{50} 0.008 ± 0.001 μM respectively).

3.5. Cytotoxicity and pro- & anti-inflammatory interleukin levels in LPS induced macrophages

The cell viability of macrophages (J774A.1) was evaluated using pyrazolopyridines **5g** and **5j**. Fig. 5 shows that **5g** and **5j** at concentrations of 0.5 to 10 (nM). Low concentrations (0.5–1.5 (nM)) did not affect cell viability, whereas 2 and 10 nM **5g** and **5j** did affect cell viability. Consequently, we used the concentration of 2 nM of **5g** and **5j** in subsequent experiments. The IC_{50} was found as 1.25 ± 0.001 nM. Lipopolysaccharide can elicit macrophage cells to discharge inflammatory cytokines such as TNF-α, IL-6, IL-10, and IL-1β. In the inflammation mechanism, severe tissue impairment, and septic shock due to unnecessary and uneven release of these cytokines may cause systemic inflammatory response syndrome (SIRS) [30,31]. The effect of **5g** and **5j** and Indomethacin on the production of the pro-inflammatory cytokines TNF-α, IL-1β, and IL-6 and the anti-inflammatory cytokine IL-10 was estimated in the culture medium of macrophages stimulated with 1 μg/mL of LPS alone or in combination with 2 nM of **5g** and **5j** (Fig. 6).

Pyrazolopyridines **5g** and **5j** considerably decreased TNF-α, IL-6, and IL-1β, and the properties were comparable to those attained with **5g**, **5j** and higher than Indomethacin. Furthermore, **5g** and **5j** showed an augmented IL-10 production at 2 nM concentration matched with the control group, and the increase in IL-10 production was higher than that observed in the group treated with indomethacin.

3.6. Structure activity relationship

A comparision between pyrazolopyridines (**5a-l**) inter-efficiency comparision of biological activity was analyzed to establish structure-activity relationship preliminary. Pyrazolopyridines **5a**, **5b**, **5g,** and **5j** were screened for biological activities based on their binding affinity to COX-2 in order to develop them as COX-2 inhibitors. The efficiency of inflammationmedication of the seleced compounds were evaluated over HRBC membrane stabilization and assesseing the inhibition of release of lysozyme enzymes from HRBC. In the molecular level assessment of inflammatory cytokines, we expected suppression of TNF-α, IL-1β, and IL-6 (pro-inflammatory), and induction of production of IL-6 (anti-inflammatory) in macrophages was expected. Among the compounds assessed for the above mentioned activities, **5g** (-OH substituted at 6th and 29th carbon position) and **5j** (-nitro group at 6th and 31st carbon position) signifigantly showed a dominated activity while compare with other compounds including the standard drugs used. While the compounds **5a** and **5b** were showed lesser activity than **5g** and **5j** were found with only thiophene functional unit at 1st and 24 & 25th carbon. This indicates the necessity of the functional group substitution in the thiophenecarbaldehyde that was used to substitute with intermediate (3Z,5E)-1-methyl-3,5-bis(thiophen-2-ylmethylene) piperidin-4-one (see Fig. 7).

4. Conclusion

In this study, pyrazolopyridines (**5a-l**) were synthesized by a two-step reaction as anti-inflammatory agents. In all *in vitro* and *in silico* studies, compounds **5g** and **5j** represented a dominated results in all proposed activity assessments. Along with Indomethacin, compounds **5g** and **5j** were evaluated for the levels of pro-inflammatory cytokines (TNF-α, IL-1β, and IL-6) and the anti-inflammatory TNF-α, IL-1β, and IL-6. Compounds **5g** and **5j** significantly reduced TNF-α, IL-1β, and IL-6, and the effects were similar to each other and better than with indomethacin. Furthermore, compounds **5g** and **5j** increased IL-10 production at 2 nM concentration compared with the control group, and the rise in IL-10 production was higher than that observed in indomethacin treated group. The need for further animal model and preclinical studies for **5g** and **5j** was recognized in order to develop them as future inflammation medications.

Appendix A. Supplementary material

Supplementary data to this article can be found online at https://doi.org/10.1016/j.bioorg.2019.103484.

References

[1] S. Abu-Melha, Synthesis and antimicrobial activity of some new heterocycles incorporating the pyrazolopyridine moiety, Arch. Pharm. Chem. Life Sci. 346 (2013) 912–921.
[2] N.S. El-Gohary, M.I. Shaaban, New pyrazolopyridine analogs: Synthesis, antimicrobial, anti-quorum-sensing, and antitumor screening, Eur. J. Med. Chem. 152 (2018) 126–136.
[3] P. Nagender, R.N. Kumar, G.M. Reddy, D.K. Swaroop, Y. Poornachandra, C.G. Kumar, B. Narsaiah, Synthesis of novel hydrazone and azole functionalized pyrazolo[3,4-b]pyridine derivatives as promising anticancer agents, Bioorg. Med. Chem. Lett. 26 (2016) 4427–4432.
[4] C. Cheng, P. Chuan, W. Sun, J. Wang, D. Xiao, L. Ding, H.F. Bu, Novel 2H-pyrazolo [4,3-c]hexahydropyridine derivatives: Synthesis, crystal structure, fluorescence properties and cytotoxicity evaluation against human breast cancer cells, Sci. China Chem. 56 (2013) 702.
[5] P. Supavilai, M. Karobath, The action of pyrazolopyridines as modulators of [3H] flunitra zepam binding to the GABA/benzodiazepine receptor complex of the cerebellum, Eur. J. Pharmacol. 70 (1981) 183–193.
[6] P. Hunter, The inflammation theory of disease. The growing realization that chronic inflammation is crucial in many diseases opens new avenues for treatment, EMBO Rep. 13 (2012) 968–970.
[7] M.P. Motwani, J. Newson, S. Kwong, A. Richard-Loendt, R. Colas, J. Dalli, D.W. Gilroy, Prolonged immune alteration following resolution of acute inflammation in humans, PLoS One 12 (2017) e0186964.
[8] D. Pohl, S. Benseler, Systemic inflammatory and autoimmune disorders, Handb. Clin. Neurol. 112 (2013) 1243–1252.
[9] L. Chen, H. Deng, H. Cui, J. Fang, Z. Zuo, J. Deng, Y. Li, X. Wang, L. Zhao, Inflammatory responses and inflammation-associated diseases in organs, Oncotarget 9 (2017) 7204–7218.
[10] O.D. Richard, G.G. Graham, The vascular effects of COX-2 selective inhibitors, Aust. Prescr. 27 (2004) 142–145.
[11] B. Hinz, O. Cheremina, K. Brune, Acetaminophen (paracetamol) is a selective

cyclooxygenase-2 inhibitor in man, FASEB J. 22 (2008) 383–390.
[12] K.J. Sales, H.N. Jabbour, Cyclooxygenase enzymes and prostaglandins in reproductive tract physiology and pathology, Prostaglandins Other Lipid. Mediat. 71 (2003) 97–117.
[13] E. Ricciotti, G.A. FitzGerald, Prostaglandins and inflammation, Arterioscler. Thromb. Vasc. Biol. 31 (2011) 986–1000.
[14] J.M. Cavaillon, Pro- versus anti-inflammatory cytokines: myth or reality, Cell Mol. Biol. (Noisy-le-grand) 47 (2001) 695–702.
[15] J.M. Zhang, J. An, Cytokines, inflammation, and pain, Int. Anesthesiol. Clin. 45 (2007) 27–37.
[16] P. Wojdasiewicz, Ł.A. Poniatowski, D. Szukiewicz, The role of inflammatory and anti-inflammatory cytokines in the pathogenesis of osteoarthritis, Mediators Inflamm. 2014 (2014) 561459.
[17] C.A. Anosike, O. Obidoa, L.U. Ezeanyika, Membrane stabilization as a mechanism of the anti-inflammatory activity of methanol extract of the garden egg (*Solanum aethiopicum*), Daru 20 (2012) 76.
[18] A. Manikandan, P. Moharil, M. Sathiskumar, C. Muñoz-Garay, A. Sivakumar, Therapeutic investigations of novel Indoxyl-based indolines: a drug target validation and Structure-Activity Relationship of angiotensin-converting enzyme inhibitors with cardiovascular regulation and thrombolytic potential, Eur. J. Med. Chem. 141 (2017) 417–426.
[19] S.M. Chelli, A. Manikandan, P. Sridhar, A. Sivakumar, B.S. Kumar, R.R. Sabbasani, Drug repurposing of novel quinoline acetohydrazide derivatives as potent COX-2 inhibitors and anti-cancer agents, J. Mol. Struct. 1154 (2018) 437–444.
[20] A. Manikandan, V.P. Muralidharan, M. Andrew, M.H. Ahmed, S.K. Iyer, S. Arumugam, Computational approaches to develop isoquinoline based antibiotics through DNA gyrase inhibition mechanisms unveiled through antibacterial evaluation and molecular docking, Mol. Inf. 37 (2018) 1800048.
[21] N. Sudhapriya, A. Manikandan, M. Rajesh Kumar, P.T. Perumal, Cu-mediated synthesis of differentially substituted diazepines as AChE inhibitors; validation through molecular docking and Lipinski's filter to develop novel anti-neurodegenerative drugs, Bioorg. Med. Chem. Lett 29 (2019) 1308–1312.
[22] A. Manikandan, A. Sivakumar, Molecular docking, discovery, synthesis, and pharmacological properties of new 6-substituted-2-(3-phenoxyphenyl)-4-phenyl quinoline derivatives; an approach to developing potent DNA gyrase inhibitors/antibacterial agents, Bioorg. Med. Chem. 25 (2017) 1448–1455.
[23] A. Manikandan, S. Ravichandran, K.I. Sathiyanarayanan, A. Sivakumar, Efficacy and rationale of 2-(4-phenylquinolin-2-yl) phenols as COX-2 inhibitors; an approach to emergent the small molecules as the anti-inflammatory and analgesic therapeutics, Inflammopharmacology 25 (2017) 621–631.
[24] M. Rajesh Kumar, A. Manikandan, V.D. Victor, Synthesis, characterization and molecular evaluation of substituted indoline based dihydroxy-thiocarbamides as selective COX-2 inhibitors, J. Heterocyclic Chem. 55 (2018) 1658–1668.
[25] A. Manikandan, S. Ravichandran, K. Kumaravel, A. Sivakumar, R. Priya, Molecular docking and in vitro evaluations of Hippocampus trimaculatus (seahorse) extracts as anti-inflammatory compounds, Int. J. Bioinf. Res. Appl. 12 (2016) 355–371.
[26] A. Manikandan, S.C. Nemani, V. Sadheeshkumar, S. Arumugam, Spectroscopic investigations for photostability of Diclofenac sodium complexed with hydroxypropyl-β-cyclodextrin, J. App. Pharm. Sci. 6 (2016) 098–103.
[27] C.C. Alves, C.F. Da Costa, S.B. De Castro, T.A. Correa, G.O. Santiago, R. Diniz, A.P. Ferreira, M.V. De Almeida, Synthesis and evaluation of cytotoxicity and inhibitory effect on nitric oxide production by J774A.1 macrophages of new anthraquinone derivatives, Med. Chem. 9 (2013) 812–818.
[28] G. Liang, S. Yang, L. Jiang, Y. Zhao, L. Shao, J. Xiao, F. Ye, Y. Li, X. Li, Synthesis and Antibacterial Properties of Mono-carbonyl Analogues of Curcumin, Chem. Pharm. Bull. 56 (2008) 162–167.
[29] C.A. Lipinski, Lead- and drug-like compounds: the rule-of-five revolution, Drug Discov. Today Technol. 1 (2004) 337–341.
[30] R. Shimazu, S. Akashi, H. Ogata, Y. Nagai, K. Fukudome, K. Miyake, MD-2, a molecule that confers Lipopolysaccharide responsiveness on Toll-like Receptor 4, J. Exp. Med. 189 (1999) 1777.
[31] B. Beutler, N. Krochin, I.W. Milsark, C. Luedke, A. Cerami, Control of cachectin (tumor necrosis factor) synthesis: mechanisms of endotoxin resistance, Science 232 (1986) 977.